IJC
International Journal of Cancer

Hypermutagenesis in untreated adult gliomas due to inherited mismatch mutations

Jason K. Sa[1,2], Seung Won Choi[1,3], Junfei Zhao[4,5], Yeri Lee[1,2], Jing Zhang[6], Doo-Sik Kong[7], Jung Won Choi[7], Ho Jun Seol[7], Jung-Il Lee[7], Antonio Iavarone[6,8,9], Raul Rabadan[4,5] and Do-Hyun Nam[1,3,7]

[1]Institute for Refractory Cancer Research, Samsung Medical Center, Seoul, Republic of Korea
[2]Research Institute for Future Medicine, Samsung Medical Center, Seoul, Republic of Korea
[3]Deparment of Health Sciences and Technology, SAIHST, Sungkyunkwan University, Seoul, Republic of Korea
[4]Department of Systems Biology, Columbia University, New York, New York, USA
[5]Department of Biomedical Informatics, Columbia University, New York, New York, USA
[6]Institute for Cancer Genetics, Columbia University, New York, New York, USA
[7]Department of Neurosurgery, Samsung Medical Center, Sungkyunkwan University School of Medicine, Seoul, Republic of Korea
[8]Department of Pathology, Columbia University, New York, New York, USA
[9]Department of Neurology, Columbia University, New York, New York, USA

Hypermutagenesis refers to marked increase in the number of mutations due to continuous mutagenic process. Hypermutated tumors, have being found in several tumor types, are associated with inherited or acquired alterations in the DNA repair pathways. Hypermutation has been observed in a subset of adult glioma patients as a direct result of temozolomide(TMZ)-induced mutagenesis. In our study, we have identified a rare subset of treatment-naïve adult gliomas with *de novo* hypermutator phenotype and explored the evolution of spontaneous and treatment-induced hypermutagenesis. We conducted Whole-Exome Sequencing (WES), Whole-Transcriptome Sequencing (WTS), and Single-Cell Sequencing (SCS) of TMZ-naïve and post-TMZ-treated hypermutated tumors to identify distinct clinical or genomic manifestations that contribute to the development of hypermutation in untreated adult gliomas. TMZ-naïve hypermutated tumors were marked by absence of *IDH1* somatic mutation and *MGMT* promoter (p*MGMT*) methylation, two genomic traits that were significantly associated with the TMZ-induced hypermutagenic event in glioblastoma, and harbored inherited alterations in the mismatch repair (MMR) machinery. The immediate family members of the TMZ-naive hypermutated glioma patients were also previous diagnosed with cancer development history, suggesting that germline dysfunction of the MMR pathway could potentially pose hereditary risk to genetic predisposition of carcinogenesis in gliomas. Lastly, both TMZ-naïve and post-TMZ-treated hypermutated tumors exhibited a significant accumulation of neoantigen loads, suggesting immunotherapeutic alternatives. Our results present new and unique understanding of hypermutagenic process in adult gliomas and an important step towards clinical implication of immunotherapy in glioma treatment.

Introduction

DNA repair mechanism is part of the essential cell homeostasis, ensuring genome integrity.[1] Alterations in the DNA repair pathways, both hereditary and somatic, largely contribute to carcinogenesis and hypermutagenesis,[2–4] manifesting specific genomic profiles and sensitivities to diverse therapies, including immunotherapy.[5–11] As the number of systematic sequencing efforts have accumulated exponentially in recent years,[12–14] prevalence of hypermutator genotype have become evident across multiple cancer types, including gliomas.[4,15,16] Glioma is the most common primary malignant brain tumor in adults.[17] The current

Key words: hypermutation, temozolomide, neoantigenicity, glioma, mismatch repair deficiency
Additional Supporting Information may be found in the online version of this article.
J.K.S. and S.W.C. contributed equally to this work.
Conflict of interest: The authors declare no competing financial interests.
Grant sponsor: Korea Health Technology R&D project through the Korea Health Industry Development Institute (KHIDI), funded by the Ministry of Health & Welfare, Republic of Korea; **Grant number:** HI14C3418
DOI: 10.1002/ijc.32054

History: Received 3 Sep 2018; Accepted 29 Nov 2018; Online 11 Dec 2018
Correspondence to: Do-Hyun Nam M.D. Ph.D., Department of Neurosurgery, Samsung Medical Center, Sungkyunkwan University School of Medicine, 81 Irwon-ro, Gangnam-gu, Seoul, Republic of Korea, Tel.: 82-2-3410-3497, E-mail: nsnam@skku.edu

What's new?

Hypermutation has been observed in a subset of adult glioma patients as a direct result of temozolomide (TMZ)-induced mutagenesis, leading to therapeutic resistance. Here, the authors identified a rare subset of pre-treatment adult glioma patients with *de novo* hypermutator phenotype. TMZ-naïve hypermutated tumors lacked somatic mutation of IDH1 and MGMT promoter methylation, and harbored both germline and somatic dysregulation of mismatch repair machinery encoding genes. Patients with TMZ-naïve hypermutagenesis demonstrated high incidence of cancer-development history in their immediate family members. Both TMZ-naïve and post-TMZ treated hypermutated tumors exhibited a significant accumulatin of neoantigen loads, pointing towards potential implementation of immunotherapy.

standard regimen for glioma patients consists of surgical resection followed by radiotherapy and/or concomitant and adjuvant temozolomide (TMZ) treatment.[18,19] TMZ has been associated with improved prognosis in overall survival of the patients, specifically those with transcriptional silencing of the O-6-Methylguanine-DNA Methyltransferase (*MGMT*) gene, mediated by promoter methylation. However, previous literatures have shown that a fraction of TMZ-treated patients acquired a hypermutator phenotype,[15,16,20] a direct result of TMZ-induced mutagenesis due to inactivation of the DNA mismatch repair (MMR) pathway, and they subsequently acquired treatment-induced therapeutic resistance.[21–24] In our study, we report a rare subset of adult glioma patients with *de novo* hypermutator phenotype with no prior therapeutic intervention. We investigate whether TMZ-naïve hypermutagenesis manifests distinct genomic or clinical features that present secondary mutagenic trajectory, suggesting potential alternative avenue for malignant transformation.

Materials and Methods

Clinical manifestations and glioma specimens

With appropriate approval from the institutional review board, all glioma specimens were obtained from patients undergoing surgery at the Samsung Medical Center. The study protocol was approved by our institution's ethical committees, and written informed consents were received from all patients. After thorough analysis by pathologists, tumor specimens were snap-frozen and preserved in liquid nitrogen for genomic analysis.

Whole-exome sequencing

An Agilent SureSelect kit was used to capture exonic DNA fragments. An Illumina HiSeq 2000 instrument was used for sequencing and generating 2 x 101-bp paired-end reads.

Somatic mutation

The sequenced reads from the FASTQ files were aligned to the human genome assembly (hg19) using the Burrows-Wheeler Aligner (BWA) version 0.6.2. The initial alignment BAM files were subjected to conventional preprocessing before mutation calling: sorting, removing duplicated reads, locally realigning reads around potential small indels and recalibrating base quality scores using SAMtools, Picard version 1.73 and Genome Analysis ToolKit (GATK) version 2.5.2. We used Mutect (version 1.1.4) and Somatic IndelDetector (GATK version 2.2) to distinguish high-confidence predictions on somatic mutations between neoplastic and non-neoplastic tissue pairs. Variant Effect Predictor (VEP) was used to annotate the acquired somatic mutations.

Copy number alteration

ngCGH python package was used to generate estimated copy number alterations. The patient-matched normal WES data were used as reference to distinguish copy number changes in tumor specimens. The gene was labeled as "amplified" when the copy number was 3 or higher and "deleted" when it was 1.5 or lower.

Bulk RNA sequencing

RNA-seq libraries were prepared using the Illumina TruSeq RNA Sample Prep kit. Sequenced reads were subjected to quality trimming and mapped onto hg19 using GSNAP, not allowing mismatch, indels, or splicing. The resulting alignments were sorted and summarized into BED files using SAMtools and bedTools. The BED files were used to calculate values of RPKM (reads per kilobase of transcript per million reads) for each gene, using DEGseq package.

Isolation of single cells for RNA sequencing and single-cell analysis

We used the C1TM Single-Cell Auto Prep System (Fluidigm) with the SMARTer kit (Clontech) to generate cDNAs. Cells were captured as a single isolate on a C1 chip, determined from bright-field images under 100× magnification using the Axiovert200 inverted microscope (Carl Zeiss). Libraries were generated using the NexteraXT DNA Sample Prep Kit (Illumina) and sequenced on the HiSeq 2,500 using 100-bp paired-end mode of the TruSeq Rapid PE Cluster kit and the TrueSeq Rapid SBS kit. Subsequent RNA reads were filtered at Q33 using Trimmomatic-0.30 and mapped to reference. For single-cell analysis, we filtered out non-neoplastic cells based on transcriptome profiles. We employed the expression signatures of normal astrocytes, oligodendrocytes, neurons, microglia and other immune cells to classify individual cells according to their expression profiles. We further validated our annotation of malignant cells from non-malignant cells using the CONICSmat package to infer large-scale copy number variations (CNVs) from single-cell RNA-seq data.

Glioma-intrinsic transcriptional subtype analysis

To estimate glioma-intrinsic transcriptional subtype, we evaluated single sample Gene Set Enrichment Analysis (ssGSEA) for each subtype markers. Each corresponding subtype scores were normalized and the subtype with the highest z-score within each sample was assigned as its dominant subtype identity.

HLA typing

HLA typing for each sample was performed using POLYSOLVER algorithm.[25]

Somatic mutation immunogenicity predictions

We used the pVAC-Seq pipeline with the NetMHCcons binding strength predictor to identify neoantigens.[26] NetMHCcons integrates three state-of-the-art methods NetMHC, NetMHCpan and PickPocket to give the most accurate predictions.[26] As required, we used the variant effect predictor from Ensembl to annotate variants for downstream processing by pVAC-Seq.[27] For each single-residue missense alteration, MHC binding affinity was predicted for all the wild-type and mutant peptides of 8, 9, 10 and 11 amino acids in length. Based on widely accepted standards of the field, mutant peptides with binding affinity of <500 nM and corresponding wild-type peptides with binding affinity >500 nM were considered as a predicted binder. The mutant peptide with the strongest binding affinity was selected for neoantigen counts.

MGMT promoter methylation

DNA was extracted from tumor tissue specimens using the QIAamp DNA Mini Kit (Qiagen) and the resulting DNA was modified with sodium bisulfite treatment using the EpiTect Bisulfite Kit (Qiagen). Afterward, the CpG island region of the *MGMT* was amplified and assessed using methylation/unmethylation specific primers. Methylation; TTTCGACGTT CGTAGGTTTTCGC (forward) and GCACTCTTCCGAAAAC GAAACG (reverse). Unmethylation; TTTGTGTTTTGATG TTTGTAGGTTTTTGT (forward) and AACTCCACACTCTT CCAAAAACAAAACA (reverse).[28,29] Additionally, the reactions were validated by electrophoresis to verify the methylation status of the *MGMT* promoter. PCR products were 81 bp (methylation) and 93 bp (unmethylation), respectively.

Results

Genomic characterization of TMZ-naive and TMZ-treated hypermutated tumors

To assess distinct genomic characteristics of TMZ-naïve hypermutated gliomas, we identified 14 patients (7 TMZ-naïve and 7 TMZ-treated) with a hypermutator phenotype among 243 patients whose Whole-Exome Sequencing (WES) of both tumor specimens and matched normal blood were available (Table 1 and Fig. 1*a*). All hypermutated tumors exhibited extremely large numbers of non-synonymous somatic mutations with average of 98.2 mutations/Mb, significantly exceeding the average number of mutation rates found in non-hypermutated tumors (Fig. 1*a*). Patients with post-TMZ-treated hypermutated tumors have undergone 6 to 18 cycles of temozolomide treatment. Both TMZ-naïve and post-TMZ-treated cases showed somatic alterations in the core oncogenic pathways that are frequently dysregulated in glioblastoma including p53, Rb and receptor tyrosine kinase (RTK)/Ras/Phosphoinositide 3-kinase (PI3K) signaling pathways. Furthermore, glioma-intrinsic transcriptional subtype analysis revealed high prevalence of proneural cellular state in both groups (Fig. 1*b*). Consistent with prior notions that *IDH1*-mutated tumors are more susceptible to acquiring a hypermutator phenotype,[15,20] majority of the TMZ-treated tumors were marked by somatic mutations in *IDH1*, while all TMZ-naïve tumors demonstrated absence of *IDH1* mutation ($P = 0.02$, Fisher's exact test) (Fib. 1b).

Table 1. Clinical information of patients who were diagnosed with either treatment-naïve or treatment-received hypermutated gliomas

Patient Clinical Information				
Patient	**Sex**	**Age**	**Pathology**	**Prior Tx**
BT101[1]	Male	68	GBM	None
BT102[1]	Female	40	GBM	None
BT103	Male	45	AA	None
BT104[1]	Female	21	GBM	None
BT105	Female	34	GBM	None
BT106[1]	Female	72	GBM	None
BT107[1]	Female	63	GBM	None
BT108	Female	56	AODG	RT + TMZ# 12
BT109	Female	56	GBM	RT + TMZ#6
BT110	Male	57	AA	RT + TMZ# 18
BT111	Female	53	AODG	RT + TMZ#9
BT112	Male	45	GBM	RT + TMZ# 17
BT113	Female	59	GBM	CCRT+TMZ#6
BT114	Male	24	GBM	CCRT+TMZ#6

AODG: Anaplastic Oligodendroglioma; GBM: Glioblastoma; AA: Anaplastic Astrycoma; RT: radiotherapy; CCRT: concurrent chemoraditionary therapy; TMZ: temozolomide.
[1]Patients had family history of malignant tumors.

Previous studies have identified a subset of GBM tumors with characteristic DNA methylation profile, commonly known as glioma CpG island methylator phenotype (G-CIMP).[30,31] The global methylator phenotype is often induced by the gain-of-function *IDH1* mutation at arginine 132 and the resulting tumors frequently demonstrate molecular and clinical features that are distinct from Non-G-CIMP tumors. The hypermethylation of the genome in G-CIMP tumors often encompass the promoter region of the O^6-methylguanine-DNA methyltransferase (*MGMT*) gene. Subsequently, p*MGMT* methylation attributes to impairment of DNA repair mechanism[32] and development of a hypermutator phenotype. Consistent with the previous reports, majority of the post-TMZ-treated hypermutated tumors demonstrated aberrant DNA methylation of the p*MGMT* (Fig. 1*b*) followed by attenuated mRNA expression level (Supporting Information Fig. S1). Conversely, TMZ-naïve tumors mainly exhibited unmethylated p*MGMT* status.

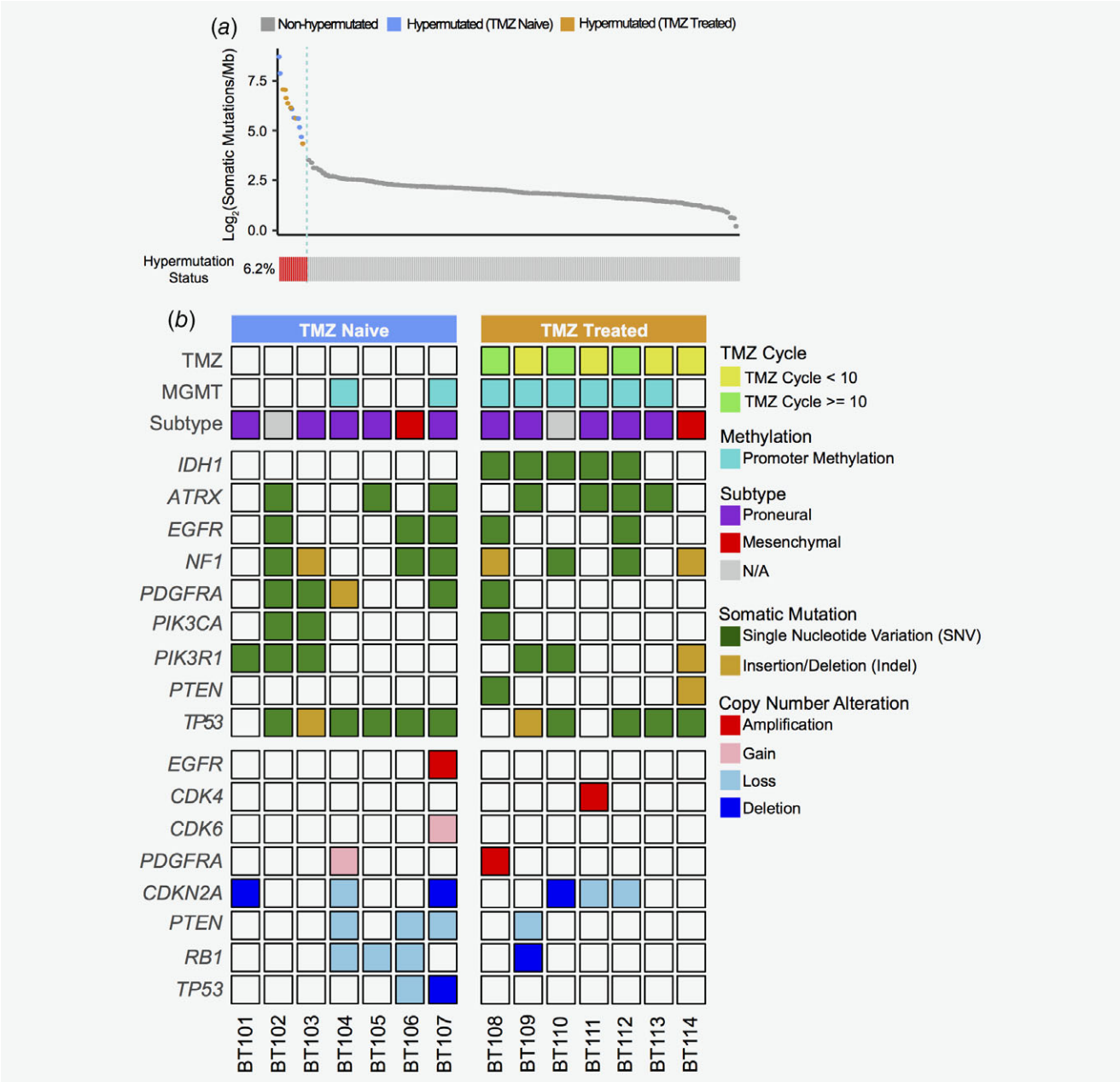

Figure 1. Genomic landscape of TMZ-naïve and TMZ-treated hypermutated gliomas. (*a*) Somatic mutational frequencies in TMZ-naïve and TMZ-treated hypermutated high-grade gliomas compared to non-hypermutated high-grade gliomas. Data on the *y* axis are log-transformed. (*b*) Genomic landscape of TMZ-naïve and TMZ-treated hypermutated gliomas. Number of TMZ cycle, *MGMT* promoter methylation status, glioma-intrinsic transcriptional subtype, somatic alterations including single nucleotide variation (SNV) and small insertion/deletion (Indel), and copy number alterations are shown for each corresponding patient.

Collectively, our results suggest that TMZ-naïve hypermutated tumors follow an alternative evolutionary path in acquiring a hypermutator phenotype.

Dysregulation of mismatch repair (MMR) machinery

DNA mismatch repair mechanisms are composed of various essentials, necessary for maintaining genome integrity and faithful replications. Mismatch repair (MMR) safeguards genome integrity through correcting improper nucleotide pairings that arise from replication errors. Dysfunction of the MMR largely contributes to accumulation of spontaneous mutations during tumor progression. Both TMZ-naïve and TMZ-treated tumors acquired somatic mutation of the MMR encoding genes including MSH (*MSH2*, *MSH3*, *MSH5*, *MSH6*; 12/14 tumors), MLH (*MLH1*, *MLH3*; 7/14 tumors) and/or PMS family (*PMS1*, *PMS2*; 5/14 tumors) (Fig. 2*a*). We also

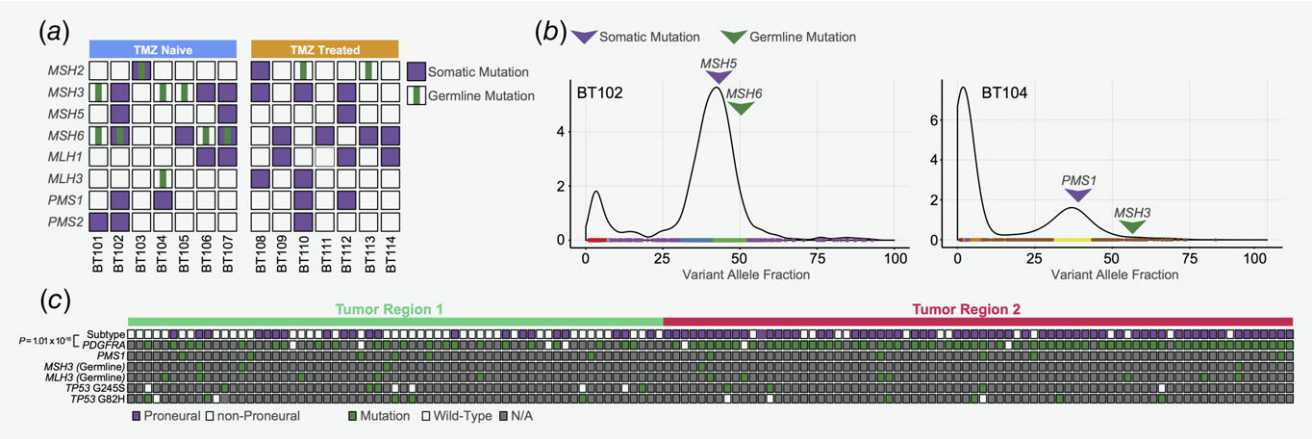

Figure 2. Dysregulation of mismatch repair (MMR) encoding genes. (*a*) Germline and somatic mutation of the MMR encoding genes in TMZ-naïve and TMZ-treated hypermutated tumors. The panel includes patients for whom whole-exome sequencing data of both tumor and matched normal specimens were available. (*b*) Variant allele fractions of both somatic and germline MMR mutations are portrayed with respect to all other mutations in the genome. (*c*) Subtype expression phenotype and mutational profiles of individual tumor cells from patient, BT104 are shown. For each tumor cell, the subtype with the highest enrichment score was determined as the corresponding identity; Proneural (Purple) and non-Proneural (White). *PDGFRA*, *PMS1*, *MSH3*, *MLH3* and *TP53* genomic alterations could be identified in the single-cell expression data (green), despite the abundance of missing data (gray). The *p* value for co-occurence of the Proneural subtype and *PDGFRA* mutation were obtained using the hypergeometric test.

identified nonsynonymous germline mutations of the MMR associated genes in the TMZ-naïve tumors, including *MSH2, MSH3, MSH6* and *MLH3*. Lynch syndrome, an autosomal dominant genetic condition that is characterized by germline alterations in the MMR genes, is associated with increased risk of carcinogenesis including colon and endometrial cancers.[33–35] As these genetic conditions are often hereditary, we expanded clinical assessment of the patients with germline MMR variations to their immediate family members. As suspected, several members of the patients' families were previously diagnosed with cancer development history including brain tumor, lung, breast and prostate carcinomas. Consistently, several germline mutations have been formerly associated with cancer predisposing syndromes including rs63749919, (*MSH6,* Y969C), rs55740729, (*MSH6,* K1358D) and rs1114167705 (*MSH6,* F1088S). We postulated that combined inherent and somatic mutations of the mismatch repair genes were integral to the rapid progression of a hypermutator phenotype in TMZ-naïve tumors, demonstrating a secondary pathway that drive hypermutagenesis in gliomas. Furthermore, we observed that the mismatch repair mutations were clonally represented in the tumors (high allelic fraction >35%), suggesting an explosive accumulation of somatic mutations after acquiring MMR pathway disruption (Fig. 2*b*).

To further interrogate the clonality of TMZ-naïve hypermutated tumors at a single cell level, we curated single-cell sequencing data from multi-region tumor samples (main mass and resection margin) from an individual patient (BT104). To distinguish non-malignant from malignant cells, we first employed the expression signatures of stromal and immune cells to classify individual cells based on their transcriptome profiles. Afterward, we estimated inferred copy-number variations for individual cells using gene expression profiles over large chromosomal regions within each cell. Each tumor cell demonstrated large-scale chromosomal aberrations, including amplification of chromosome 8 and deletions of 5,10 and 13 (Supporting Information Fig. S2). On the contrary, cells that were classified as non-malignant cells lacked any detectable CNVs. Consistent with the bulk WES results, mutations of the MMR encoding genes including, *PMS1*, *MLH3* and *MSH3,* were detected across all single cells with enough coverage at the corresponding genomic regions (Fig. 2*c*). Additionally, we also discovered a high frequency of *PDGFRA* mutations (60%, 83/138), which significantly associated with a proneural expression phenotype. These observations were consistent with the bulk WTS results, where proneural transcriptional subtype was predominant among hypermutated tumors.

Distinct mutational signatures and elevated neoantigen loads in hypermutated tumors

Next, we evaluated mutational signatures of TMZ-naïve and TMZ-treated hypermutated tumors.[36,37] Of the six classes of base substitution in the mutation type, both groups exhibited robust presence of C-to-T transition (Fig. 3*a*). TMZ-naïve tumors were characterized by prominence of C-to-T substitutions at NpCpG trinucleotides (where N represents any nucleotide), which has been speculated to be a direct result of elevated rate in spontaneous deamination of 5-methylcytosine[38] (Fig. 3*b*). On the other hand, post-TMZ treatment tumors were enriched with excess C-to-T substitutions at NpCpC and NpCpT trinucleotides, which is an evident indication of TMZ-induced mutagenesis[36,37] (Fig. 3*b*). Notably, majority of the driver mutations that were observed in the post-TMZ treatment tumors consist

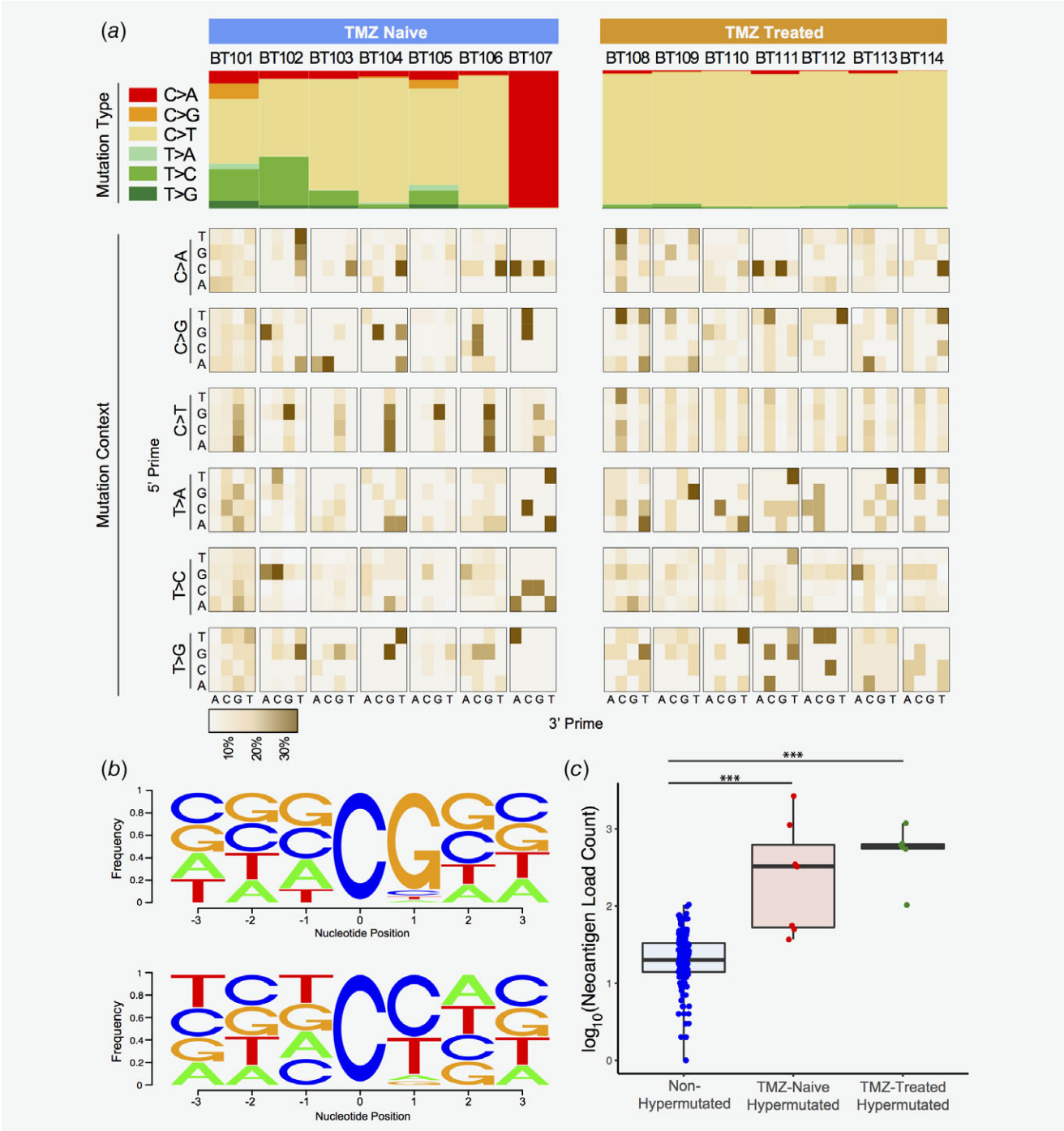

Figure 3. Mutational transition of TMZ-naïve and TMZ-treated hypermutated tumors. (*a*) Top panel exhibits mutational type, indicating mutational spectrum of each hypermutated tumors. Bottom panel notes mutational context, demonstrating base substitution mutation spectra of each somatic mutation. All 96 mutated trinucleotides are represented in a heatmap. The base corresponding to 5′ is shown on the vertical axis and the 3's base is on the horizontal axis. (*b*) Representative nucleotide context of the C-to-T transitions in TMZ-naïve (upper panel) and TMZ-treated (bottom panel) hypermutated tumors. The height of the letters represents the occurrence frequency of the corresponding nucleotide at each position. (*c*) Log-scaled Neoantigen load counts in non-hypermutated, TMZ-naïve hypermutated, and TMZ-treated hypermutated tumors. *P*-values were calculated using the Wilcoxon rank sum test. ***$P < 0.001$.

of C-to-T substitutions at NpCpC and NpCpT contexts, suggesting that these tumors have undergone TMZ-induced malignant progressions.

High mutational burden has been shown as an integral indication of neoantigen production and presents potential immunotherapeutic intervention across multiple cancer types.[6,8,9,39]

Therefore, we have assessed neoantigenicity levels in both TMZ-naïve and post-TMZ-treated hypermutated tumors compared to non-hypermutated tumors. Notably, both hypermutated tumors exhibited a significant accumulation of neoantigen load (Fig. 3*c*), suggesting potential immunotherapeutic strategy for these patients.

Discussion

In our study, we report for the first time a group treatment-naïve adult glioma patients with a hypermutator phenotype and explore their spontaneous genomic profiles that constitute an alternative mutagenic process. Notably, TMZ-naïve hypermutated tumors were primarily marked by absence of *IDH1* somatic mutation and p*MGMT* methylation, two genomic features that were significantly associated with development of hypermutation in GBM.[16] Transcriptional silencing of *MGMT* gene *via* promoter methylation, followed by dysfunction of the MMR encoding genes were presumably the underlying mechanism behind TMZ-induced hypermutator phenotype.[12,40,41] Furthermore, hypermutagenesis in glioma has been exclusive to recurrent tumors as it has been perceived as a direct result of TMZ intervention that subsequently lead to therapeutic resistance to standard treatment regimen. Therefore, it remained controversial whether inactivation of the MMR encoding genes or hypermutation was directly associated with acquisition of TMZ-induced resistance. Our results have shown that spontaneous *de novo* hypermutated tumors follow an alternative evolutionary trajectory in acquiring continuous mutagenic process *via* combination of germline and somatic mutations of the mismatch repair genes. Despite having such features, patients with *de novo* hypermutation exhibited favorable clinical responses to the standard TMZ chemotherapy (Supporting Information Fig. S3), in contrast to the previous notion that inactivation of *MSH6* could potentially confer TMZ resistance in glioblastoma.[24] Although recent literatures have identified multiple brain tumor types to be associated with Lynch syndrome MMR mutational carriers, including *MLH1* and *MSH2*,[42–44] TMZ-naïve patients primarily demonstrated high prevalence *MSH3* and *MSH6* germline variations. Our results suggest that inherited dysfunction of the MMR pathway through *MSH3* or *MSH6* mutation could potentially pose hereditary risk to genetic predisposition of carcinogenesis. Our speculations were further corroborated *via* expanded evaluation of the patients' clinical history. Notably, patients with TMZ-naïve hypermutator phenotype demonstrated a significantly higher incidence of cancer-related occurrences in their immediate family members (Supporting Information Table S1). These observations suggest that inherited mutations in the MMR encoding genes could potentially promote tumor initiation and further impairment of the DNA repair mechanism *via* newly acquired somatic variation could result in hypermutation development.

A substantial body of evidence has highlighted significant association between patients with elevated neoantigen load and improved clinical response to checkpoint-blockade immunotherapy across various cancer types including glioblastoma.[6–9,39] Interestingly, our results showed increased neoantigen counts in both TMZ-naïve and post-TMZ-treated hypermutated tumors, suggesting potential implication of checkpoint inhibitors in these patients. Even though hypermutagenesis in a newly-diagnosed glioma is a rare event, it is important that all patients should to be evaluated for a hypermutated genotype as early identification of glioma patients prior to temozolomide treatment could potentially lead to new clinical trials in evaluating replacement of alkylating agents with checkpoint inhibitors. However, further studies are warranted in implementing immunotherapeutic approach in glioma patients as CNS malignancies are often void of cytotoxic immune cells such as T cells, which are critical components in immune checkpoint inhibition. Therefore, only a subset of glioma patients could be appropriate targets for immunotherapeutic approach in defined scenarios, such as presence of a hypermutator phenotype. As such, our results provide a conceptual groundwork for clinical practice against glioma patients with *de novo* hypermutation.

Although complete understanding of the underlying mechanism behind spontaneous hypermutagenesis in glioma requires an in-depth experimental validation, we demonstrate that combined inherent and somatic mutations of the mismatch repair encoding genes could largely contribute to development of *de novo* hypermutator phenotype in gliomas. Furthermore, our results present an important step towards potential implementation of immunotherapy in glioma treatment.

Acknowledgements

The biospecimens for our study were provided by Samsung Medical Center BioBank.

References

1. Hanahan D, Weinberg RA. Hallmarks of cancer: the next generation. *Cell* 2011;144: 646–74.
2. Cancer Genome Atlas Research Network, Kandoth C, Schultz N, et al. Integrated genomic characterization of endometrial carcinoma. *Nature* 2013;497:67–73.
3. Cancer Genome Atlas Research Network. Comprehensive molecular characterization of human colon and rectal cancer. *Nature* 2012; 487:330–7.
4. Campbell BB, Light N, Fabrizio D, et al. Comprehensive analysis of Hypermutation in human cancer. *Cell* 2017;171:1042–56.
5. Van Allen EM, Miao D, Schilling B, et al. Genomic correlates of response to CTLA-4 blockade in metastatic melanoma. *Science* 2015;350:207–11.
6. Johanns TM, Miller CA, Dorward IG, et al. Immunogenomics of Hypermutated Glioblastoma: a patient with Germline POLE deficiency treated with checkpoint blockade immunotherapy. *Cancer Discov* 2016;6:1230–6.
7. Bouffet E, Larouche V, Campbell BB, et al. Immune checkpoint inhibition for Hypermutant Glioblastoma Multiforme resulting from Germline Biallelic mismatch repair deficiency. *J Clin Oncol* 2016;34:2206–11.
8. Le DT, Uram JN, Wang H, et al. PD-1 blockade in tumors with mismatch-repair deficiency. *N Engl J Med* 2015;372:2509–20.
9. Rizvi NA, Hellmann MD, Snyder A, et al. Cancer immunology. Mutational landscape determines sensitivity to PD-1 blockade in

non-small cell lung cancer. *Science* 2015;348: 124–8.
10. Dietlein F, Thelen L, Reinhardt HC. Cancer-specific defects in DNA repair pathways as targets for personalized therapeutic approaches. *Trends Genet* 2014;30:326–39.
11. Manic G, Obrist F, Sistigu A, et al. Trial watch: targeting ATM-CHK2 and ATR-CHK1 pathways for anticancer therapy. *Mol Cell Oncol* 2015;2: e1012976.
12. Cancer Genome Atlas Research. N. Comprehensive genomic characterization defines human glioblastoma genes and core pathways. *Nature* 2008;455:1061–8.
13. Cancer Genome Atlas Research. N. Integrated genomic analyses of ovarian carcinoma. *Nature* 2011;474:609–15.
14. Lee JK, Wang J, Sa JK, et al. Spatiotemporal genomic architecture informs precision oncology in glioblastoma. *Nat Genet* 2017;49:594–9.
15. Johnson BE, Mazor T, Hong C, et al. Mutational analysis reveals the origin and therapy-driven evolution of recurrent glioma. *Science* 2014;343: 189–93.
16. Wang J, Cazzato E, Ladewig E, et al. Clonal evolution of glioblastoma under therapy. *Nat Genet* 2016;48:768–76.
17. Louis DN, Perry A, Reifenberger G, et al. The 2016 World Health Organization classification of tumors of the central nervous system: a summary. *Acta Neuropathol* 2016;131:803–20.
18. Furnari FB, Fenton T, Bachoo RM, et al. Malignant astrocytic glioma: genetics, biology, and paths to treatment. *Genes Dev* 2007;21: 2683–710.
19. Stupp R, Mason WP, van den Bent MJ, et al. Radiotherapy plus concomitant and adjuvant temozolomide for glioblastoma. *N Engl J Med* 2005;352:987–96.
20. Kim J, Lee IH, Cho HJ, et al. Spatiotemporal evolution of the primary Glioblastoma genome. *Cancer Cell* 2015;28:318–28.
21. Cahill DP, Levine KK, Betensky RA, et al. Loss of the mismatch repair protein MSH6 in human glioblastomas is associated with tumor progression during temozolomide treatment. *Clin Cancer Res* 2007;13:2038–45.
22. Felsberg J, Thon N, Eigenbrod S, et al. Promoter methylation and expression of MGMT and the DNA mismatch repair genes MLH1, MSH2, MSH6 and PMS2 in paired primary and recurrent glioblastomas. *Int J Cancer* 2011;129:659–70.
23. Hunter C, Smith R, Cahill DP, et al. A hypermutation phenotype and somatic MSH6 mutations in recurrent human malignant gliomas after alkylator chemotherapy. *Cancer Res* 2006;66:3987–91.
24. Yip S, Miao J, Cahill DP, et al. MSH6 mutations arise in glioblastomas during temozolomide therapy and mediate temozolomide resistance. *Clin Cancer Res* 2009;15:4622–9.
25. Shukla SA, Rooney MS, Rajasagi M, et al. Comprehensive analysis of cancer-associated somatic mutations in class I HLA genes. *Nat Biotechnol* 2015;33:1152–8.
26. Karosiene E, Lundegaard C, Lund O, et al. NetMHCcons: a consensus method for the major histocompatibility complex class I predictions. *Immunogenetics* 2012;64:177–86.
27. McLaren W, Gil L, Hunt SE, et al. The Ensembl variant effect predictor. *Genome Biol* 2016;17:122.
28. Esteller M, Garcia-Foncillas J, Andion E, et al. Inactivation of the DNA-repair gene MGMT and the clinical response of gliomas to alkylating agents. *N Engl J Med* 2000;343:1350–4.
29. Esteller M, Hamilton SR, Burger PC, et al. Inactivation of the DNA repair gene O6-methylguanine-DNA methyltransferase by promoter hypermethylation is a common event in primary human neoplasia. *Cancer Res* 1999;59:793–7.
30. Noushmehr H, Weisenberger DJ, Diefes K, et al. Identification of a CpG Island methylator phenotype that defines a distinct subgroup of glioma. *Cancer Cell* 2010;17:510–22.
31. Turcan S, Rohle D, Goenka A, et al. IDH1 mutation is sufficient to establish the glioma hypermethylator phenotype. *Nature* 2012;483: 479–83.
32. Liu L, Gerson SL. Targeted modulation of MGMT: clinical implications. *Clin Cancer Res* 2006;12:328–31.
33. Ponz De Leon M, Bertario L, Genuardi M, et al. Identification and classification of hereditary non-polyposis colorectal cancer (lynch syndrome): adapting old concepts to recent advancements. Report from the Italian association for the study of hereditary colorectal tumors consensus group. *Dis Colon Rectum* 2007;50:2126–34.
34. Meyer LA, Broaddus RR, Lu KH. Endometrial cancer and lynch syndrome: clinical and pathologic considerations. *Cancer Control* 2009;16: 14–22.
35. Jang E, Chung DC. Hereditary colon cancer: lynch syndrome. *Gut Liver* 2010;4:151–60.
36. Alexandrov LB, Nik-Zainal S, Wedge DC, et al. Signatures of mutational processes in human cancer. *Nature* 2013;500:415–21.
37. Lawrence MS, Stojanov P, Polak P, et al. Mutational heterogeneity in cancer and the search for new cancer-associated genes. *Nature* 2013;499:214–8.
38. Pfeifer GP. Mutagenesis at methylated CpG sequences. *Curr Top Microbiol Immunol* 2006;301: 259–81.
39. McGranahan N, Furness AJ, Rosenthal R, et al. Clonal neoantigens elicit T cell immunoreactivity and sensitivity to immune checkpoint blockade. *Science* 2016;351:1463–9.
40. Bodell WJ, Gaikwad NW, Miller D, et al. Formation of DNA adducts and induction of lacI mutations in big blue Rat-2 cells treated with temozolomide: implications for the treatment of low-grade adult and pediatric brain tumors. *Cancer Epidemiol Biomarkers Prev* 2003;12: 545–51.
41. van Thuijl HF, Mazor T, Johnson BE, et al. Evolution of DNA repair defects during malignant progression of low-grade gliomas after temozolomide treatment. *Acta Neuropathol* 2015;129:597–607.
42. Gylling AH, Nieminen TT, Abdel-Rahman WM, et al. Differential cancer predisposition in lynch syndrome: insights from molecular analysis of brain and urinary tract tumors. *Carcinogenesis* 2008;29:1351–9.
43. Barrow E, Robinson L, Alduaij W, et al. Cumulative lifetime incidence of extracolonic cancers in lynch syndrome: a report of 121 families with proven mutations. *Clin Genet* 2009;75:141–9.
44. Vasen HF, Stormorken A, Menko FH, et al. MSH2 mutation carriers are at higher risk of cancer than MLH1 mutation carriers: a study of hereditary nonpolyposis colorectal cancer families. *J Clin Oncol* 2001;19:4074–80.